The Journal of the Korean Society of Oceanography
Vol. 30, No. 4, pp. 237-249, August 1995

Structures and Variability of the T-S field and the Current across the Korea Strait

YOUNG JAE RO[1], MOON-JIN PARK[1], SANG-RYONG LEE[2] AND JAE CHUL LEE[3]
[1]*Dept. of Oceanography, Chungnam Natl. Univ, Taejon, Korea*
[2]*Dept. of Oceanography, Pusan Natl. Univ., Pusan, Korea*
[3]*Dept. of Oceanography, National Fisheries Univ. of Pusan, Pusan, Korea*

대한해협 횡단면 상의 수온-염분과 해류의 구조 및 변동

노영재[1] · 박문진[1] · 이상룡[2] · 이재철[3]
[1]충남대학교 해양학과
[2]부산대학교 해양과학과
[3]부산수산대학교 해양학과

To understand the cross-sectional structures of temperature, salinity and current across the Korea Strait, field measurements were carried out for the period of May 2 to 20, 1994. Using the R/V Tam Yang, detailed CTD profiles and ADCP records were obtained and used to examine the mean and variability field on two time scales (15 days and 25 hours).

A sharp coastal front in the middle of the Korea Strait exists across which two different water masses, *i. e.*, warm and saline water in the eastern side and cold and less saline water in the western side are neighboring. We observed highly variable field of T and S apparently caused by the westward movement of warm and saline water mass. Short-term fluctuations of T and S in the middle layer are remarkable and their importance was analysed as the first Eigen mode accounting for more than 50% of total variances.

The currents in the Korea Strait are strongly influenced by tidal currents with spring and neap variation whose maximum speed ranges 80-90 and 60-70 cm/s respectively near the central portion of the channel. Strong southward tidal current could even mask the Tsushima Current completely. Results of harmonic analysis show that the magnitudes of semidiurnal, diurnal and mean components of currents are comparable to each other at spring and neap tide conditions. The volume transport across the western channel of the Korea Strait were estimated to be 2.1 Sv at neap tide condition and 3.4 Sv at spring tide condition.

대한 해협 횡단면 상의 수온, 염분 및 해류의 구조를 이해하기 위하여 1994년 5월 2일부터 20일 까지 현장 조사를 수행하였다. 연구선 탐양호를 이용하여 상세한 CTD 수직 profile과 ADCP 측정 기록을 얻었으며 두 개의 시간자 (15일과 25시간)에 대한 平均場과 變動場을 분석하였다.

대한 해협 중앙부에는 서로 다른 두개의 水塊, 즉 동측의 高溫 高鹽水와 서측의 低溫 低鹽水가 서로 隣接하면서 대단히 뚜렷한 연안 전선을 형성하고 있다. 이 고온 고염 수괴가 약 보름에 걸쳐서 西進하면서 수온 염분장을 크게 변화시키고 있음을 관찰할 수 있었다. 또한 중층에서는 數時間 대의 짧은 주기로서도 수온과 염분이 변화하고 있었으며 이 현상은 EOF 분석에서 제 1고유 모드로 나타나며 그것은 50% 이상의 전체 분산을 점하고 있다.

대한 해협에서의 흐름은 조류에 의해서 심하게 영향을 받고 있으며 해협 중앙부에서 사리와 조금 때 각 각 최대 80-90 및 60-70 cm/s의 크기를 보여 준다. 강한 남향의 조류에 의해 때에 따라서는 북향하는 대마 난류의 존재가 완전히 가려 보이지 않기도 하였다. 25시간 연속 해류 관측 결과의 調和 分析 결과 사리와 조금 때 평균, 半日周潮流 및 一日周潮流의 크기가 서로 비슷함을 알 수 있었다. 대한 해협 서수도를 통과하는 容積 輸送量은 조금 때 2.1 사리 때에 3.4 Sv으로 추정되었다.

*이 논문은 1993년도 교육부 학술연구조성비(해양, 수산과학분야, 과제명: 한국 동해 연안역의 해류 구조 조사 연구)에 의하여 연구되었음.

INTRODUCTION

To understand the circulation in the entire East Sea, one should inevitably understand the current structure and its variability in the Korea Strait, which impose a most important boundary condition to the East Sea. Despite keen interests in this area, direct measurements of current and T-S distributions have been very much limited so far, that only a few direct current measurements in the Korea Strait can be listed such as KORDI(1981), Lie and Byun(1985) and Lie *et al.*(1989). ADCP measurements by Byun(1988, 1989, 1990) and Kaneko *et al.*(1991) are notable. The effects of tide in this area were studied by Lee(1970), Miita(1976), Odamaki(1989) and Choi *et al.*(1994) discuss the tide and tidal currents in the Strait.

The tide in the Korea Strait shows standing wave type and thus sea level and currents are about 90 degrees out of phase (Odamaki, 1989). The tide at Pusan is mainly semidiurnal and the amplitude of the diurnal tide is about 10% of that of the semidiurnal tide. Thus, the diurnal inequality of the tide is small. However, the diurnal component of the tidal currents in the western channel of the Korea Strait is comparable to the semidiurnal component (Odamaki, 1989), and the diurnal inequality of the tidal currents is expected to be large. The tidal current ellipse is elongated and the major axis is parallel to the western channel of the Strait.

While the transport of the Tsushima current is known to show seasonal variation, few studies so far attempted to examine the effect of spring-neap tidal variation on the Tsushima Current. Thus we put emphasis on the direct measurements of currents covering the neap-spring tidal phase in the Korea Strait.

In this study, we concentrated on the field measurements in which we obtained the detailed CTD profiles and ADCP records across the Korea Strait. The sampling strategy is described in detail.

Three main objectives can be summarized as 1) to investigate the T-S structure across the Korea Strait in terms of the space and time variability, 2) to investigate the current structure through the Korea Strait in terms of the space and time variability, 3) to investigate the interactions between T-S field and current field.

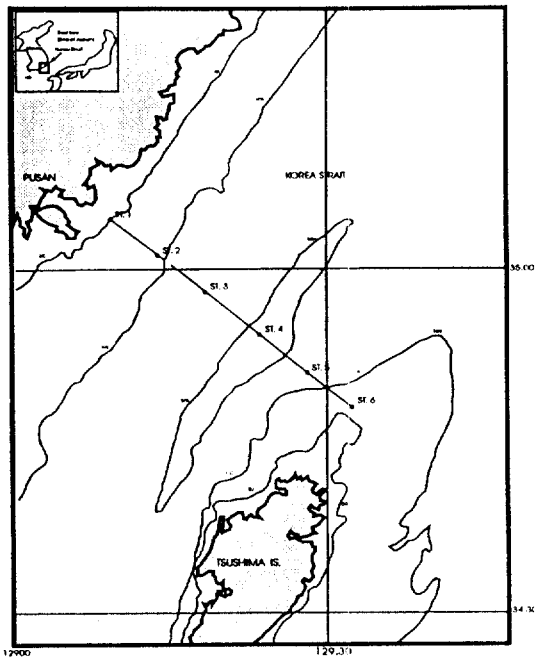

Fig. 1 The study area and the ADCP transect line with the CTD profiling stations in May, 1994.

FIELD MEASUREMENTS

To obtain the detailed T-S and current field in the Korea Strait. a transect line was chosen from Pusan to the northern tip of the Tsushima Island with 6 CTD casting stations, shown in Fig. 1. The field works have been made for the period of May 2 to 20, 1994 which covers the neap and spring tidal cycle. They were made by use of the CTD (Sea Bird 911) profiler and ADCP (RD Instrument Narrow Band Acoustic Doppler Current Profiler 150 kHz) mounted on the R/V Tam Yang. The detailed calendar field schedule is summarized in Table 1. To obtain an instantaneous picture of T-S distribution and current field, field work was designed not to last more than 4 hours to cover a transect.

CTD profilings were made at the predesignated 6 stations while the current were measured along the

Table 1. Schedule of the field work of CTD profilings and ADCP trackings in May, 1994

Date May, 1994	Time	Survey Direction	Measurement Item	Tide at Pusan		
				Time	Sea Level	Phase
2	10:00-13:30	E	ADCP	7:04	29	Neap
	14:31-17.38	W	CTD+ADCP	13:20	85	
				19:23	103	
9	09:37-12:48	E	ADCP	07:34	29	Spring
	13:53-17:32	W	CTD+ADCP	13:27	12	
12	09:51-	at St. 3	25-hour continuous CTD+ADCP	09:10	109	
13	11:52-			14:59	11	
				21:33	121	
				03:30	13	
				09:43	109	
13	14:45-18:17	S	ACDP	15:30	14	
				11:06	119	
16	08:56-13:27	E	CTD+ADCP	05:20	26	Medium
	13:36-16:02	W	ADCP	11:32	99	
				17:20	29	
19	09:16-	at St. 3	25-hour continuous CTD+ADCP	08:29	33	
20	10:36			14:52	89	
				21:00	39	
				03:26	95	
				09:43	29	
20	13:08-16:45	W	ADCP	16:18	95	

E: Eastward, W: Westward

transect line with the cruising speed optimally set around 9 knots. To understand the temporal variability of T-S and current field in the Strait, on May 12 and 19, 1994, 25-hour continuous CTD profilings were carried out to yield time series records of T and S with 2 hour sampling interval, while current measurements were simultaneously carried out.

The current observation was designed to catch the spring-neap variation of the tidal current in the Korea Strait and its effects on the Tsushima Current. Current records were obtained for the whole water column except surface and bottom layers of about 9 meters with vertical resolution of 4 meters and sampling interval of 5.5 seconds. The current velocity and direction from ADCP were averaged over 500 m horizontal interval to remove small scale disturbances and used for the subsequent analysis.

T-S STRUCTURES

Characteristics of the Cross-sectional Distribution of T and S

The characteristical distribution of T-S vertical structures can be viewed by the mean field of temperature and salinity prepared by 5-day ensemble averaging, shown in Fig. 2. Its feature is as follows; 1) warm and saline waters lies in the eastern portion of the cross-section (toward Tsushima Island), 2) a sharp coastal frontal boundary exists at the central portion between St. 3 and 4, 3) very saline waters (> 34.5 psu) occupy as core in the middle layer. Two water masses, one from cold and fresh coastal water and the other, warm and saline water which is presumably derived from the Kuroshio form a very sharp frontal boundary. This feature might be considered as ordinary mean field. However, it turned out to be not as simple and stationary, when we examine the temporal evolution of T-S field. To show this feature, daily salinity distribution in Fig. 3 are compared and watch for the saline water mass (>34. 6 psu) lying in the middle laver of St. 4. 5. and 6 on

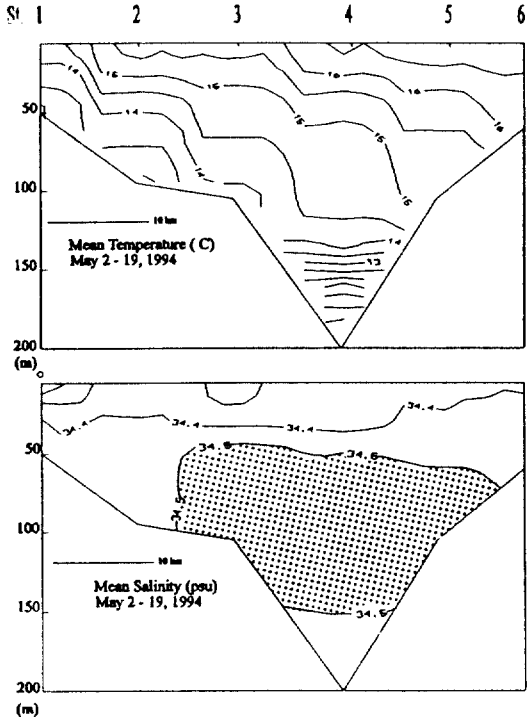

Fig. 2. Mean cross sectional distributions of the temperature and salinity in the Korea Strait from May 2 to 20, 1994.

May 2, 1994 and moving toward the western section (note the shaded area in Fig. 3). The volume occupied by this saline water mass is also changing from May 2 to 19, 1994, as it gradually moved toward west with the volume shrinking and finally diminished on May 19, 1994. This feature indicates that highly variable and active dynamical processes are undergoing in this area and contributing to T-S variability. The meandering of the coastal front (Lee *et al.*, 1984) and penetrating eddy seen in Plate 1 seem to contribute to this variability. In this aspect, such a dynamical mechanism needs to be understood for the future study.

To assess the variability of temperature and salinity, the standard deviation defined by using the ensemble mean of those are shown in Fig. 4. It shows that the variability is getting bigger toward upper layer and inshore side for both of temperature and salinity. To be noteworthy, the behaviors of the standard deviations of temperature and salinity look

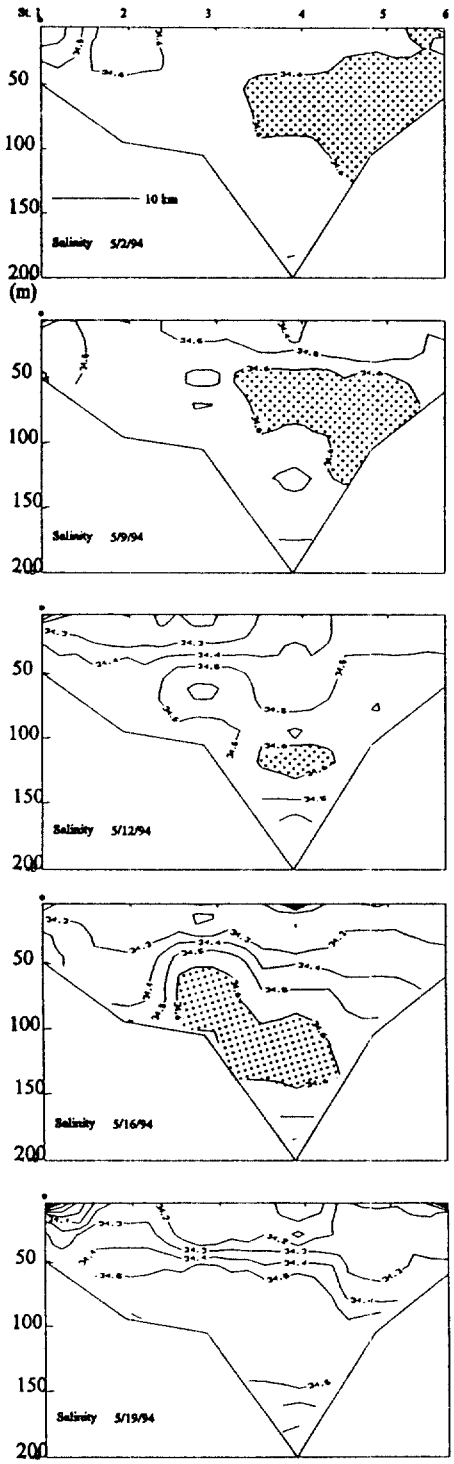

Fig. 3. Daily cross sectional distribution of salinity from May 2 to 19, 1994 in the Korea Strait.

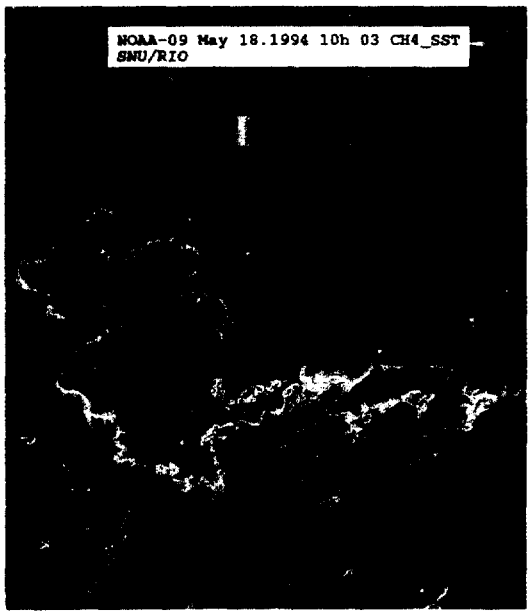

Plate 1. NOAA-9 Satellite Image showing the sea surface temperature around the Korean Peninsula on May 18, 1994.

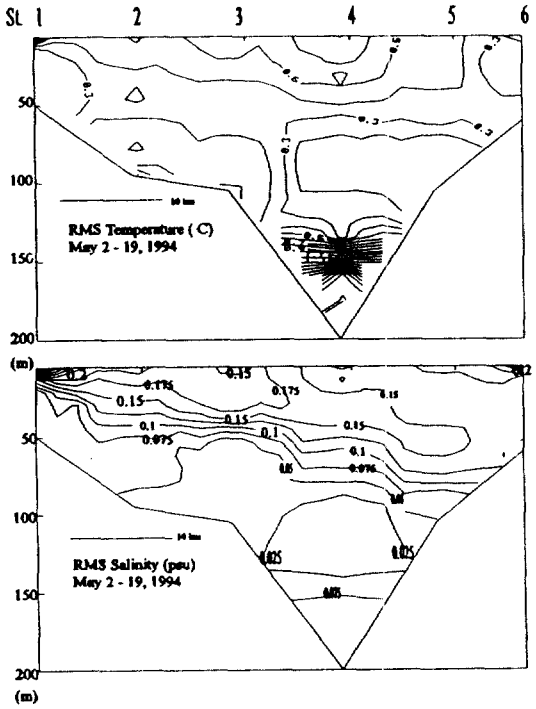

Fig. 4. The distribution of rms of temperature and salinity in the Korea Strait from May 2 to 19, 1994.

similar. In particular, the variability of temperature and salinity at St. 4 below the depth of 150 meters appears to be extraordinarily big. In fact, the temperature and salinity decrease amount to be more than 7°C and 0.25 psu, respectively from May 2 to 19, 1994. This fact indicates that through the deep channel of the Korea Strait, vigorous exchange of water is occurring between Korean Proper Water and warm and saline water from the Kuroshio.

Temporal Variability of T-S Field

In this study, we could examine the temporal variability of temperature and salinity on two time scales, ie, 17 days (from May 2 to 19) and 25 hours which correspond to fortnightly and diurnal tidal scales. Firstly, the day-to-day variability of T-S field is obvious in Table 2 which shows that the daily means and standard deviations of temperature and salinity are changing. The standard deviations of T-S on May 12 and 19 are bigger than those on the other dates. The reason is not obvious, yet. It is not coincident with neap (May 2) and spring (May 12) tidal cycle, either. The big variabilities of T-S in

Table 2. Statistics of cross-sectional distibution of temperature and salinity in the Korea Strait in May, 1994

Date	Temperature(°C)				
	Mean	S.D.	Max.	Min.	Range
5. 2.	14.78	1.23	16.79	12.62	4.17
5. 9.	14.62	1.42	17.08	10.32	6.76
5. 12	14.51	2.08	17.42	8.44	8.98
5. 16	14.55	1.57	16.18	7/44	8.74
5. 19	14.56	2.48	17.90	6.27	11.63
Date	Salinity(psu)				
5. 2.	34.57	0.07	34.64	34.20	0.44
5. 9.	34.52	0.08	34.67	34.36	0.31
5. 12.	34.44	0.13	34.63	34.17	0.46
5. 16.	34.31	0.15	34.62	34.11	0.51
5. 19.	34.34	0.21	34.57	34.09	0.48

the middle layer are believed to be the result of a small scale (about ten kilometers in diameter) eddy penetration. This is clearly depicted in space-time contour plot of salinity at 45 meter depth in Fig. 5 (note the arrow direction showing the westward (inshore) movements of saline water mass). The speed of westward movement of saline water mass agrees well with the in situ ADCP measurements

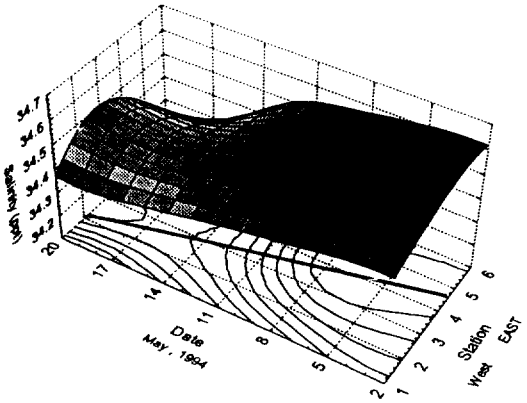

Fig. 5. Space-time contour of salinity at 45 meter depth from May 2 to 19, 1994 in the western channel of the Korea Strait.

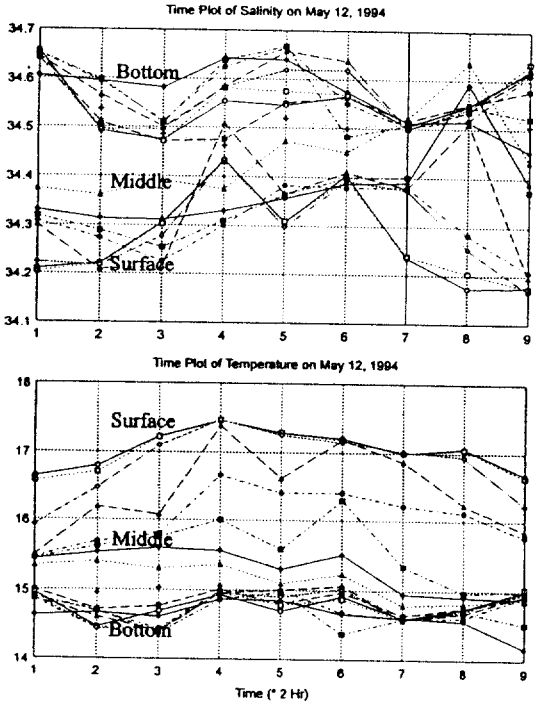

Fig. 6. Time plot of temperature and salinity of May 12, 1994. at St. 3 in the middle of western channel of the Korea Strait.

which has about 10 cm/s inshore velocity on May 19, 1994. We believe that this phenomenon is the most prominent and important one discovered by the in situ CTD and ADCP measurements for this study.

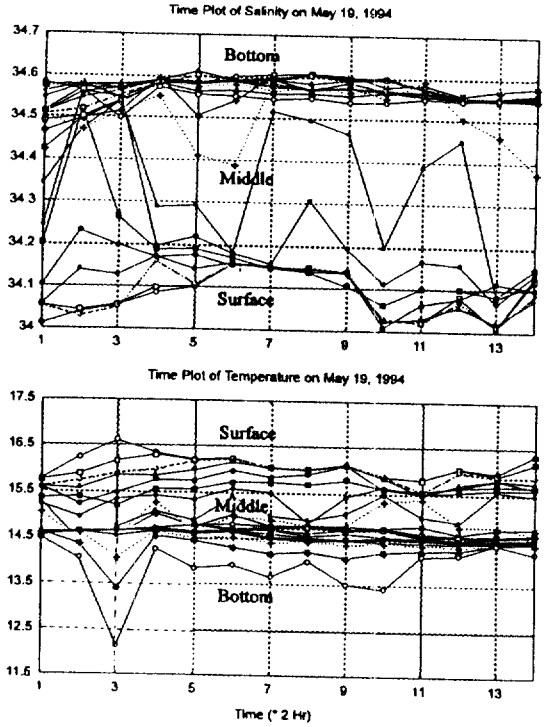

Fig. 7. Time plot of temperature and salinity on May 19, 1994. at St. 3 in the middle of western channel of the Korea Strait.

Secondly, for the variability of T-S on diurnal time scale, Fig. 6 and 7 show the time plots of T-S from surface to bottom with 5 meter-depth-interval. Fig. 8 and 9 show the time mean vertical profiles of T-S with minimum and maximum values on May 12 and 19, 1994. By visual inspections, the temporal behaviors of T-S can be grouped into three layers (surface, middle and bottom). This fact is clearly reflected in the following correlation and Empirical Orthogonal Function (EOF) analysis. Statistics of temporal variability of T-S at three layers are summarized in Table 3. It is noteworthy that the biggest variability occurs in the middle layer near the thermocline and the halocline (25-40 meters) rather than in the surface (note the shaded area in Figs 8 and 9). The standard deviation value of 0.5°C exists in the middle layer, while 0.1 to 0.3°C lies in the surface and bottom layers. As noted earlier in space variability, the behaviors of temperature and salinity variability are similar to each other. In the middle

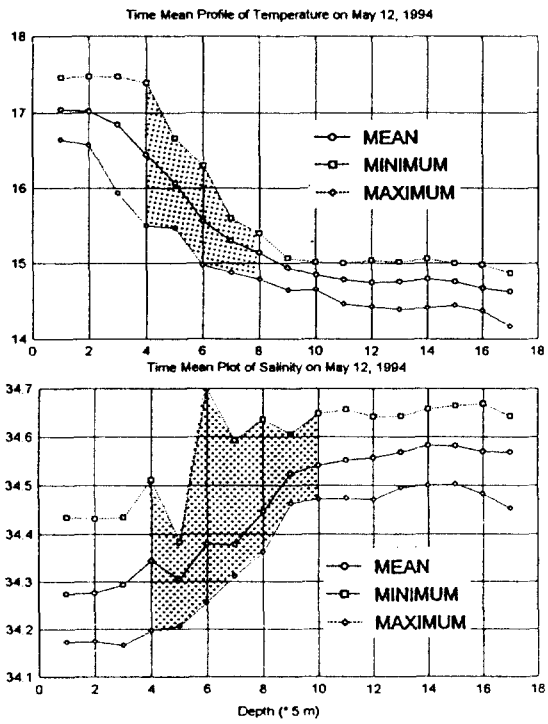

Fig. 8. Time mean vertical profile of temperatures and salinities on May 12, 1994. at St. 3 in the middle of western channel of the Korea Strait.

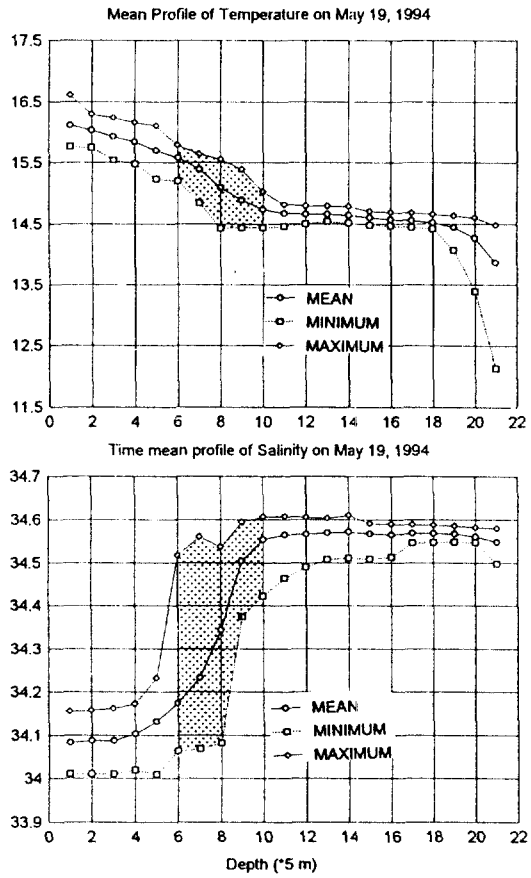

Fig. 9. Time mean vertical profile of temperatures and salinities on May 19, 1994. at St. 3 in the middle of western channel of the Korea Strait.

layer (here between 30 and 60 meter in depth), very sharp haloclines exist which are more prominent than thermocline. To show this variability associated with the middle layer more closely, in Fig. 8, we pay attention to the salinity variations at the depths of 25 to 45 meters with 0.2 to 0.3 psu jumps with the time scale of 4 to 6 hours. We regard this as a result of either vigorous eddy activities with short time scale or the internal tide. This phenomena seem to happen through the undulation of the halocline (pycnocline) so that lower saline waters penetrate into upper middle layer intermittently.

EOF characteristics of T and S Temporal Variations

The time series data base, 9 samples at 17 depths on May 12 and 14 samples at 21 depths of temperature and salinity were subject to the EOF analysis. The temporal behavior of temperature and salinity at various depths can be easily understood in terms of several dominant Eigen modes. Among the results derived from this analysis, Table 3 summarizes the important ones.

In general, three Eigen modes are dominant explaining about 90% of the total variances of T and S variations, respectively. In Table 3, the percentage contributions of the Eigen modes for the total variances are shown. On the whole, more than 50% of the variances of T and S can be explained by the first Eigen mode, respectively. In Table 3, the Depth indicate the depth ranges of T or S at which the Eigen modes are dominant explaining the variances. For example, the salinity variance on May 19, 1994 is explained by the first Eigen mode by 53%

Table 3. Statistics and the results of the EOF analysis.

Result of Statistical Analysis					
Date	Layer	Temperature (°C)		Salinity (psu)	
		Mean	S.D.	Mean	S.D.
5. 12	surface	16.49	0.01	34.312	0.059
	middle	14.95	0.23	34.500	0.066
	bottom	14.72	0.22	34.574	0.064
5. 19.	surface	15.86	0.20	34.111	0.065
	middle	14.90	0.21	34.461	0.086
	bottom	14.53	0.11	34.567	0.019
Result of EOF Analysis					
Date	Eigen Mode	contr. (%)	Depth (m)	contr. (%)	Depth (m)
5. 12.	1	60	10~25	38	25~35
	2	15	30~45	31	0~20
	3	13	50~75	18	50-75
5. 19.	1	33	25~45	53	20~35
	2	28	0~20	23	40~60
	3	13	90~95	13	0~15

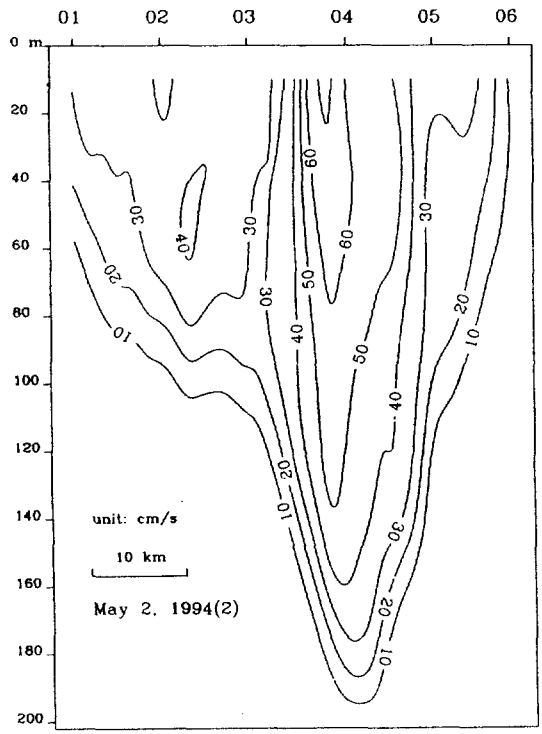

Fig. 10. Sectional velocity across the western channel of the Korea Strait on May 2, 1994 (neap tide condition).

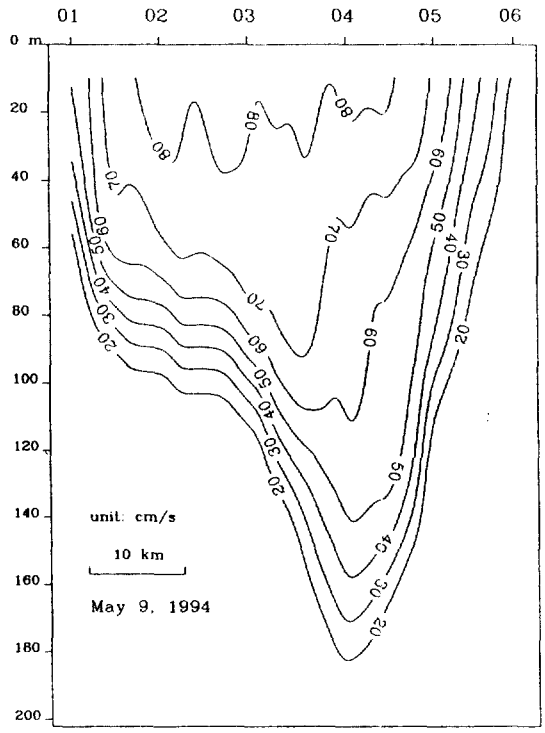

Fig. 11. Sectional velocity across the western channel of the Korea Strait on May 9, 1994 (neap tide condition).

and the mode is particularly dominant in the depth range of 20 to 35 meters. The EOF analysis indicates that the first Eigen mode explains the variances of T and S in the subsurface and/or middle layer, while the second or third mode is associated with the variability of the T and S at surface or bottom layer. In another words, the variability of T-S in the middle layer is bigger than those in other layers.

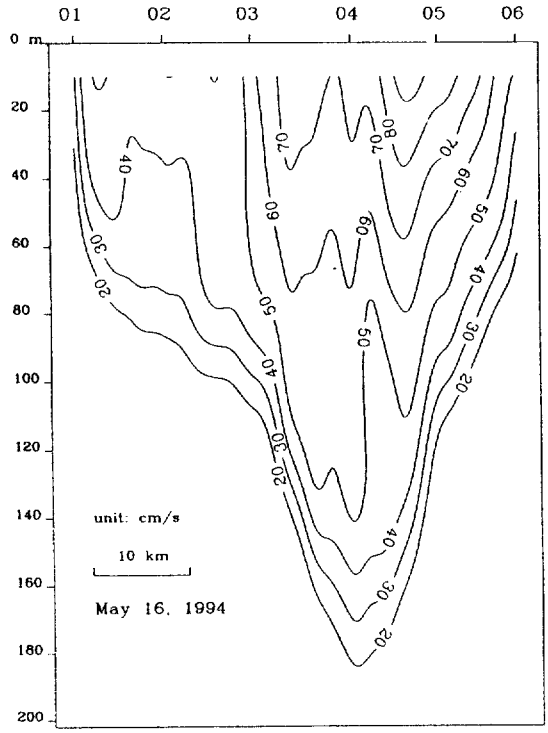

Fig. 12. Sectional velocity across the western channel of the Korea Strait on May 16, 1994 (medium tide condition).

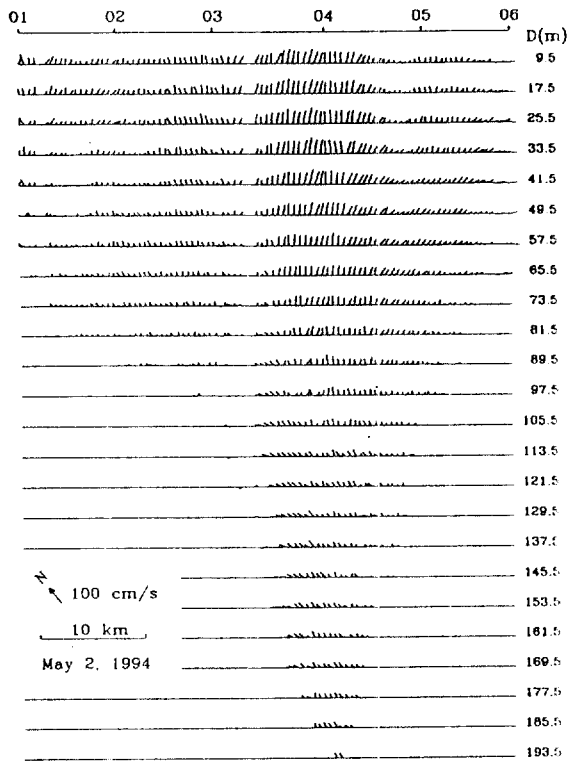

Fig. 13. Current structure at the western channel of the Korea Strait on May 2, 1994.

The processes occurring in the middle layer are out of phase with those in the surface and bottom layers and thus result in the negative correlations of temperature and salinity between surface and middle layer, respectively. In particular for the salinity on May 19, 1994, we could distinguish the big negative correlations between surface and middle layer values.

CURRENT STRUCTURE

Tidal Effect on the Tsushima Current

The flow structures in the western channel of the Korea Strait in Fig. 10, 11 and 12 correspond to neap, spring and medium tide conditions, respectively. These sectional views of the current velocity were measured for 2 to 3 hours from 1 to 2 hours after the high water at Pusan. The temporal variation of the ebb current velocity around the maximum ebb currents showed only about 10% variation of speed with almost same direction for about 3 hours. All three figures (10, 11, 12) show that the flow is generally northeastward at all depths. The maximum current velocities normal to the transect are 80 to 90 cm/s for the spring tide, 70 to 80 cm/s for the medium tide, and 60 to 70 cm/s for the neap tide condition.

At the neap tide condition on May 2, 1994, the velocity of the main stream is about 60 to 70 cm/s which is confined near St. 4 at the center of the channel. The secondary core of the velocity exists near St. 2 from 40 to 60 m depth where relatively broad shelf with gentle bottom slope is located. Also, strong horizontal velocity shear is found between St. 3 and 4. The velocity structure of the medium tide condition on May 16, 1994 shows the mixed pattern of those at neap and spring tide conditions.

At the spring tide condition on May 9, 1994, the sectional velocity over 80 cm/s extends between St.

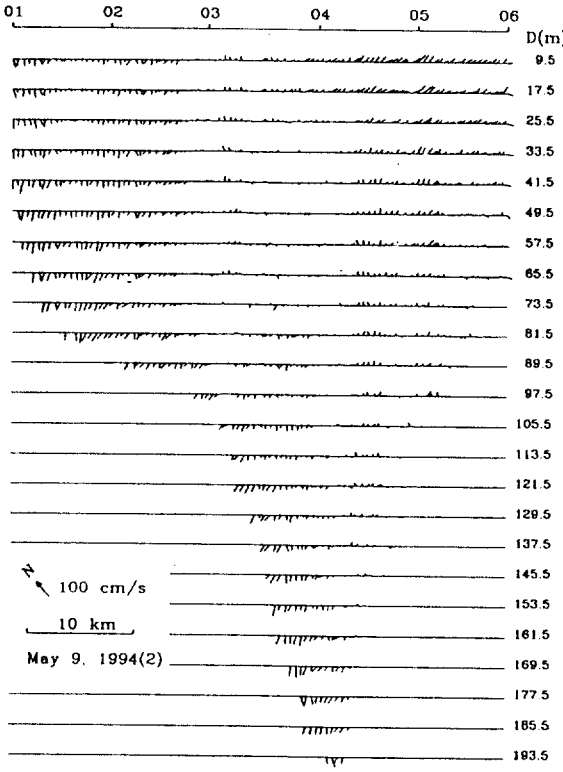

Fig. 14. Current structure at the western channel of the Korea Strait on May 9, 1994.

2 and 4 and persists down to about 40 m depth. It gradually decreases to 60 cm/s at 100 m and 50 cm/s at 140 m depth near St. 4 which is deepest in the channel. Below 140 m in depth, the current velocity decrease rapidly down to less than 20 cm/s at 190 m depth. From St. 5 to 6, the current direction gradually changes from northeastward to eastward and the sectional velocity decreases rapidly to about 20 cm/s at St. 6.

The effect of the flood tidal current which flows southwestward opposing the Tsushima Current is shown for the neap tide condition in Fig. 13 and for the spring tide condition in Fig. 14. The current velocities in Fig. 13 are observed for 3.5 hours from about 3 hours after the low water at Pusan. The flood current seems not strong enough to reverse the current velocity on May 2 (Fig. 13). At spring tide, however, the flood tidal current can smear out the northeastward Tsushima Current as shown in Fig. 14. The southwestward flow is stronger at the deep trough and near the coast where weak Tsushima Current is expected.

Harmonic Analysis of the Current

Continuous current measurements on May 12 and 19, 1994 (see examples in Fig. 15) were subject to the harmonic analysis as follows ;

$$vi(t) = v_o + v_1\cos(\omega_1 t + \phi_1) + v_2\cos(\omega_2 + \phi_2)$$

where vi denotes for i-th depth current velocity and v_o, v_1, and v_2 represent mean, diurnal and semidiurnal components of current. with their frequencies and phase lags, (ω_1, ϕ_1, and ω_2, ϕ_2). Due to the limited data length, we could not seperate the M_2 and S_2 or K_1 and O_1 tidal constituents.

Results of harmonic analysis on 25 hour Eulerian current measurements are shown in Fig. 16. At both spring and neap tide conditions, the magnitudes of semidiurnal, diurnal and mean current are comparable to each other throughout the water column. Here, the mean current includes not only non-tidal

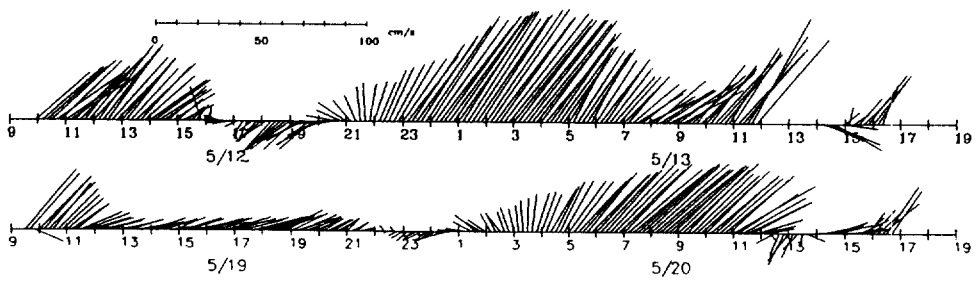

Fig. 15. Typical example of time series record of current in the Korea Strait on May 13 and 20, 1994.

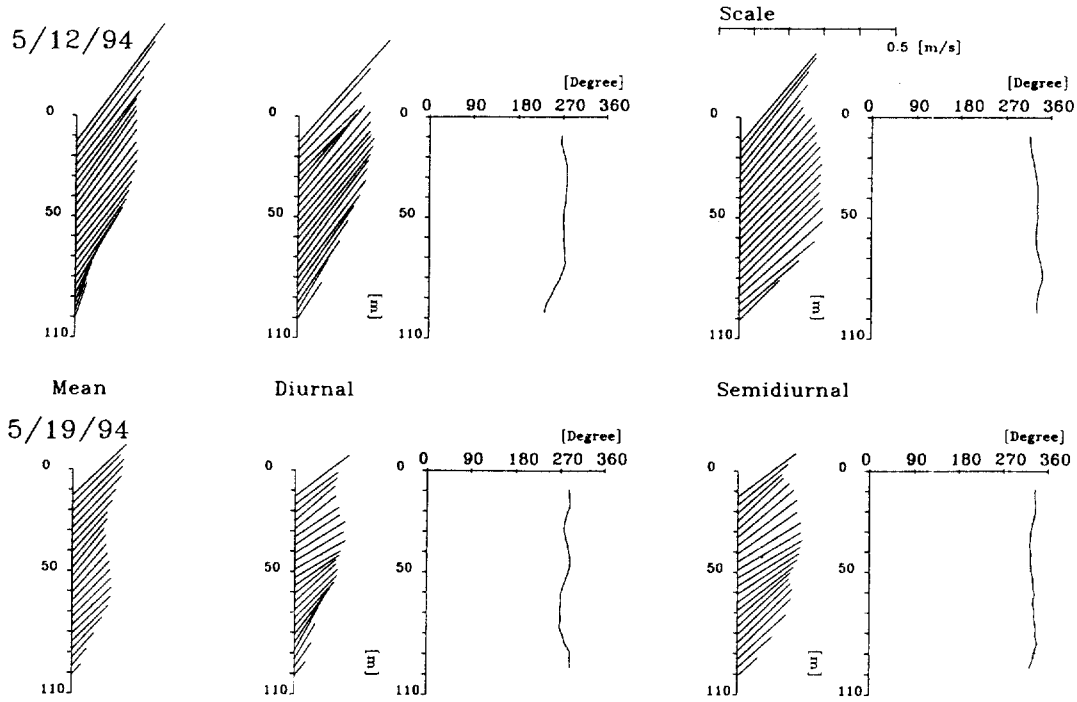

Fig. 16. Results of the harmonic analyses of the 25-hour continuous current measurements for the mean, diurnal and semidiurnal components at the various depths.

part, but tidal current of over 25 hour period. The magnitude of each component is generally 30 to 40 cm/s at spring tide, and 20 to 25 cm/s at neap tide at upper part of the water column. The direction of each component is largely northeast-southwestward regardless of the spring and neap tidal conditions. It is noteworthy that the current speeds and directions are more or less uniform throughout the water column except surface and near-bottom. This implies that the barotropic component of the current is bigger than the baroclinic component. The velocity in the surface and bottom layers might be influenced by other forcings from eddy penetration and bottom friction.

Geostrophic Current Computations

The database from the CTD profilings for five days was used for the computations of the geostrophic currents in the study area. The method used was traditional one (Pond and Pickard, 1974) with the reference level at 110 to 140 meters due to the data limitations.

The results of the geostrophic computations show the day-to-day variations in that surface current decreases with depth and its maximum speed does not exceed 30 cm/s which is less than half of the ADCP measurements. This results is not so surprising, because the current measured by ADCP contains the barotropic component as well as baroclinic ones. Out of five geostrophic computations, we only present Fig. 17 on May 9, 1994, which shows a good agreement in the general pattern where strong current core exists in the upper middle channel. On the spring tide on May 9, 1994, the geostrophic current shows the southward flow which is masked by the strong southward flood current (not shown).

Volume Transport in the Western Channel of the Korea Strait

From the spatial and temporal current ob-

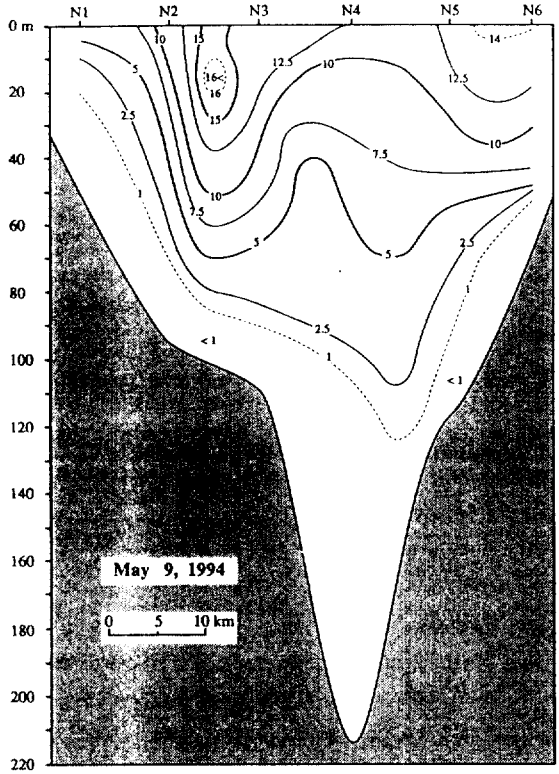

Fig. 17. Cross sectional distribution of the geostrophic velocity estimated from the CTD profilings in the western channel of the Korea Strait on May 9, 1994. Compare this to the current pattern in Fig. 11.

servations, we found that the tidal component greatly influence the volume transport across the western channel of the Korea Strait and the barotropic component of the current dominates over the baroclinic component. The total volume transports across the western channel of the Korea Strait were estimated to be 3.4 Sv (May 9), 2.1 Sv (May 2) and 2.9 Sv (May 16) for spring, neap and medium tide conditions, respectively. It showed about 60% increase from neap to spring tide condition. The geostrophic volume transports calculated from the density distribution with the level of no motion at 110 to 140 m depth are only 0.3 Sv on May 9, 0.4 Sv on May 2, and 0.3 Sv on May 16, and they do not show much variation during spring-neap cycle. These values are comparable to 0.6 Sv in May by Yi(1966) who calculated the geostrophic volume transport across the Korea Strait.

SUMMARY AND CONCLUSIONS

The mean field of T and S in the Korea Strait in May, 1994 can be characterized in terms of a frontal boundary lying in the middle of the channel, across which warm and saline water mass occupies the offshore area and cold and less saline water mass exists in the inshore area. The vertical structures of T and S can be characterized in terms of three (namely surface, middle and bottom) layers where strong thermocline and halocline were formed in the middle layer. In the deep channel at St. 4, we observed very big standard deviations of both T and S which might be the result of the cold water (Korea Proper Water) intrusion from the East Sea. However, this simple picture turns out to be very much complicated, when we consider the big day-to-day variability of T and S.

We investigated the variability of the T and S in terms of two time scales, ie, 15 days and 25 hours. The long-term variability was associated with the westward movement of saline water mass. The saline water mass on May 2, 1994 occupying the eastern water column moved toward the west (inshore) in the middle layer until May 19, 1994 and the salinity higher than 34.6 psu was being diluted as a result of mixing with less saline inshore water during the movement. The short-term variability was characterized such that the fluctuations of T and S are bigger in the middle layer than in surface and bottom layers. The behaviors of the variability of T and S in three layers are clearly understood by the EOF analysis which shows the three important Eigen modes. The first Eigen mode accounting for more than 50% total variance is associated with the variability in the middle layer, while the other two modes are associated with the variabilities at the surface and bottom layers.

The dynamical mechanism associated with the variability of T and S will need to be understood. So far, we can only suggest that the penetrating eddy formed by the local baroclinic instability along the frontal boundary is responsible for the westward

movement of saline water mass. The scale of eddy seems to be tens of kilometer. For the big variability of T and S in the middle layer, we suspect the internal tide. It would sound plausible, when we consider the strong stratification in the thermocline and/or halocline depths. To be able to answer these questions, more detailed field work with a shorter sampling interval and a longer sample will be needed.

The current structure in the western channel of the Korea Strait depends strongly on the flood/ebb and spring/neap tide conditions. With the ebb tidal flow during the spring tide, the northeastward flow over 80 cm/s appear widely over 30 km of the upper layers of the western channel of the Korea Strait. However, at neap tide condition, the current velocity over 60 cm/s is confined within about 10 km near the center of the channel with high horizontal velocity shear. Also, the current velocity below 100 m depth at spring tide is similar to that at neap tide.

With the weak flood tidal current at neap tide, the northeastward current still persist through the western channel. The strong flood current at spring tide, however, can completely smear out the northeastward current and the current in the entire cross-section flows southwestward. Since the major axis of the tidal current and the Tsushima Current are directed along the western channel of the Strait, the resulting current velocity can be estimated from their relative magnitudes.

The maximum southwestward current appears 3.5 to 4.5 hours after the low water at Pusan and the maximum northeastward current occurs 3.0 to 3.5 hours after the high water at Pusan. This suggests that the tide in the western channel of the Korea Strait is standing wave type. Whereas the tide at Pusan is semidiurnal, the tidal current in the western channel is mixed type with the magnitude of the diurnal component is comparable to that of the semidiurnal component. Accordingly, the diurnal inequality of the tidal current is large in the western channel of the Strait.

ACKNOWLEDGEMENTS

Thanks are due to the Captain J. C. Kim and his crew members of the R/V Tam Yang for their cooperations during the field works. The authors would like to express their sincere gratitude to two referees for their close readings and helpful comments.

REFERENCES

Byun, S. -K., 1988. Studies on the ocean current structure in the Korea Strait, I, KORDI, 59 pp.

Byun, S. -K., 1989. Studies on the ocean current structure in the Korea Strait,II, KORDI, 47 pp.

Byun, S. -K., 1990. Studies on the ocean current structure in the Korea Strait,III, KORDI, 34 pp.

Choi, B. H., I. K. Bang and K. H. Kim, 1994. Vertical Distribution of Tidal Current in the Korea Strait. *J. Kor. Soc. Costl. and Ocean Eng.* **6**(4):421-438

Kaneko, A, S. -K. Byun, S. -D. Chang and M. Takahashi 1991 An observation of sectional velocity structures and transport of the Tsushima Current across the Korea Strait. In: Oceanography of Asian marginal seas,edited by K. Takano, Elsevier, Amsterdam, 207-222.

KORDI, 1981. Dynamics of the coastal water along the east coast of Korea. KORDI Rep. BSPE-00036-54-1. 62 pp.

Lee, C. -K., 1970. On the currents in the western channel of the Korea Strait, *Bull. Fish. Res. Dev. Agency of Korea,* **6**: 175-231(in Korean).

Lee, J. C., J. Y. Na and S. -D. Chang, 1984. The thermohaline structure of the shelf front in the Korea Strait in early winter, *J. Oceanol. Soc. Korea,* **19**: 56-67.

Lie, H. J. and S. K. Byun, 1985. Summertime southward current along the east coast of Korea. *J. Oceanogr. Soc. Korea,* **20**: 22-27.

Lie, H. J., M. S. Suk and C. H. Kim, 1989. Observation of southeastward deep current off the east coast of Korea. *J. Oceanogr. Soc. Korea,* **24**: 63-68.

Miita, T., 1976. Tsushima Current viewed in the short-term moored current meter, *Pro. Japan. Soc. Fish. Oceanogr.,* **28**: 38-58 (in Japanese).

Odamaki, M., 1989. Tides and tidal currents in the Tsushima Strait, *J. Oceanol. Soc. Japan,* **45**: 65-82.

Pond, S. and G. L. Pickard, 1983. Introductory Dynamical Oceanography. 2nd Edition, Pergamon Press, 329 pp.

Yi, Sok-U, 1966. Seasonal and secular variations of the water volume transport across the Korea Strait, *J. Oceanol. Soc. Korea,* **1**: 7-13.

Accepted July 31, 1995